Pressure- and field-induced magnetic quantum phase transitions in TlCuCl$_3$

B Normand[1], **M Matsumoto**[2], **O Nohadani**[3], **S Wessel**[2], **S Haas**[3], **T M Rice**[2] **and M Sigrist**[2]

[1] Département de Physique, Université de Fribourg, CH-1700 Fribourg, Switzerland
[2] Theoretische Physik, ETH-Hönggerberg, CH-8093 Zürich, Switzerland
[3] Department of Physics and Astronomy, University of Southern California, Los Angeles, CA 90089-0484, USA

Abstract
TlCuCl$_3$ is a quantum spin liquid of $S = 1/2$ Cu^{2+} dimers. Interdimer superexchange interactions give a three-dimensional magnon dispersion and a spin gap significantly smaller than the dimer coupling, which is closed by an applied hydrostatic pressure of approximately 2.5 kbar or by a magnetic field of 5.6 T, offering a unique opportunity to explore both the pressure- and field-induced quantum phase transitions and their associated critical phenomena.

1. Introduction

Thallium copper chloride [1, 2] presents an insulating, quantum magnetic system of dimerized $S = 1/2$ Cu^{2+} ions. Inelastic neutron scattering (INS) measurements of the elementary magnon excitations [3] reveal strong dispersion in all three spatial dimensions, indicating significant interdimer interactions. The spin gap $\Delta_0 = 0.7$ meV is significantly smaller than the antiferromagnetic (AF) dimer superexchange parameter $J \approx 5$ meV, and the corresponding critical field $H_c = 5.6$ T is of laboratory scale [2]. Neutron diffraction measurements at fields $H > H_c$ find a field-induced AF order in the plane normal to the applied field appearing simultaneously with the uniform moment [4]. INS measurements of the magnon spectra in finite fields [5], including those exceeding H_c [6], provide dynamical information concerning the elementary excitations, particularly the linear Goldstone mode [6], in the phase of field-induced magnetic order. Oosawa *et al* [7] have shown by means of neutron diffraction under a hydrostatic pressure of 14.8 kbar that TlCuCl$_3$ has a pressure-induced magnetically ordered phase [8]. The magnetic Bragg reflections are found at reciprocal lattice points $Q = (0, 0, 2\pi)$, as in the field-induced ordered phase. Subsequent experiments suggest that the critical pressure $P_c \simeq 2.5$ kbar [9] is rather small.
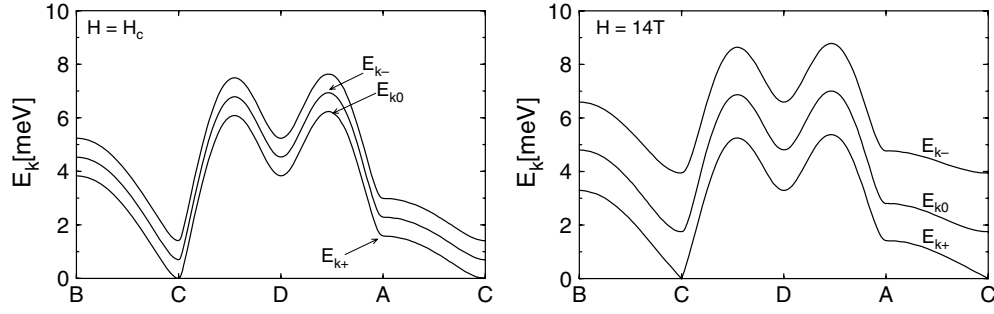
Figure 1. Dispersion of the three magnon modes in TlCuCl$_3$ using $g = 2.16$ for the g-factor. Left: $H = H_c$ (=5.6 T). Right: $H = 14$ T $> H_c$ (cf [6]).

2. Model

The dimerized TlCuCl$_3$ system is described in a finite field by the bond operators

$$s^\dagger|0\rangle = \frac{1}{\sqrt{2}}(|\uparrow\downarrow\rangle - |\downarrow\uparrow\rangle), \qquad t_+^\dagger|0\rangle = -|\uparrow\uparrow\rangle,$$
$$t_0^\dagger|0\rangle = \frac{1}{\sqrt{2}}(|\uparrow\downarrow\rangle + |\uparrow\downarrow\rangle), \qquad t_-^\dagger|0\rangle = |\downarrow\downarrow\rangle, \tag{1}$$

which are bosonic and satisfy a hard-core constraint. In the disordered regime the singlet is treated as a condensate and the dynamics described in terms of the triplet excitations [10]. The three-dimensional (3d) TlCuCl$_3$ system is described remarkably accurately by a mean-field approximation, which may thus be used with the Holstein–Primakoff expansion in which the constraint is applied in the form $s_i = \sqrt{1 - \frac{1}{N}\sum_{i,\alpha} t_{i\alpha}^\dagger t_{i\alpha}}$. This is equivalent to enforcing $\bar{s} = 1$, which results in a maximum error of 3% for TlCuCl$_3$. The magnon dispersion relations are

$$E_k = \sqrt{(\tfrac{1}{4}J - \mu + \Lambda_k)^2 - \Lambda_k^2} - \alpha h,$$
$$\Lambda_k = -\tfrac{1}{2}J_1\cos k_x - \tfrac{1}{2}J_2\cos(2k_x + k_z) + J_3\cos(k_x + \tfrac{1}{2}k_z)\cos\tfrac{1}{2}k_y, \tag{2}$$

and the exchange constants deduced for TlCuCl$_3$ [11] from the measured zero-field excitations [3] are then $J = 5.50$ meV for the dimer coupling and $J_1 = -0.43$ meV, $J_2 = 3.16$ meV, $J_3 = 0.91$ meV for the only significant interdimer exchange constants.

3. Field-induced order

The dispersion relations for the triplet magnons of the disordered phase are shown in figure 1 for the critical field $h = h_c$. The magnon bands move rigidly with field for $h < h_c$, so that the lowest mode retains its quadratic shape at the band minimum even at h_c. The condition that the lowest mode ($\alpha = +$) becomes soft at $Q = (0, 0, 2\pi)$ determines both the critical field, $h_c = g\mu_B H_c = \sqrt{J^2 - J(J_1 + J_2 + 2J_3)}$, and the static spin configuration of the ordered phase.

In the intermediate-field regime, $h_c \leqslant h \leqslant h_s$, the ordered ground state is represented [11] in the basis of equation (1) by finite expectation values $\bar{s}$, $\bar{t}_+$ and $\bar{t}_-$. A full description requires the transformation [11]

$$a_i = us_i + v(f e^{iQ\cdot r_i} t_{i+} + g e^{iQ\cdot r_i} t_{i-}), \qquad b_{i0} = t_{i0},$$
$$b_{i+} = u(f t_{i+} + g t_{i-}) - v e^{iQ\cdot r_i} s_i, \qquad b_{i-} = f t_{i-} - g t_{i+} \tag{3}$$
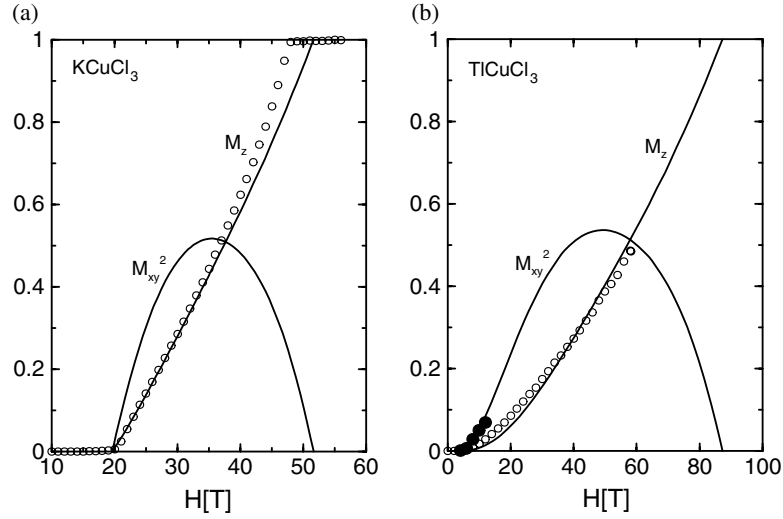
Figure 2. Normalized magnetization curves for (a) KCuCl$_3$ and (b) TlCuCl$_3$. Open circles are experimental data for M_z measured at $T = 1.3$ K, and closed circles are data for M_{xy} measured at $T = 0.2$ K. Theoretical fits are made using $g = 2.29$ for KCuCl$_3$ and $g = 2.16$ for TlCuCl$_3$.

in which the k-independent coefficients u, v, f and g arise from successive unitary transformations. The operator $a_i \longrightarrow \bar{a}$ is treated as a uniformly condensed parameter, which contains a staggered magnetization perpendicular to the field with wavevector Q. Elimination of terms linear in b minimizes the classical energy, determining the ground state, and the saturation field is given by $h_s = J + J_1 + J_2 + 2J_3$.

The spin excitations in the ordered phase are described by terms quadratic in b-operators, and are shown for a representative field $H = 14$ T in figure 1. The mode E_{k+} is always massless at the band minimum, Q, and develops a linear dependence on k in the vicinity of this point. This branch is the Goldstone mode, arising from the fact that rotation of the staggered moment about the axis of broken symmetry does not change the energy. The theoretical results show quantitative agreement with experimental measurements [5, 6] of the mode gaps and dispersion relations.

The uniform and staggered magnetization components in the ordered-phase condensate, $M_z = v^2(f^2 - g^2)$ and $M_{xy} = \sqrt{2}uv(f + g)$, are shown in figure 2 for both TlCuCl$_3$ and its structural analogue KCuCl$_3$, in which interdimer coupling is considerably weaker and the gap larger. In both cases M_{xy}^2 has linear field dependence close to H_c and to H_s, indicating that $M_{xy} \sim \sqrt{H - H_c}$ as expected from a mean-field description. By contrast, while M_z is almost purely linear (figure 2(a)) for KCuCl$_3$ (negligible mixing of the upper triplet mode t_- into the condensate, (equation (3))), a significant deviation from this form is found in TlCuCl$_3$ (figure 2(b)).

4. Pressure-induced order

A softening of magnon modes and the onset of magnetic order is also caused by increasing the interdimer interactions. This type of pressure-induced AF order has been observed [7] for the small-gap TlCuCl$_3$ system. In the disordered phase the three magnon modes are degenerate at $H = 0$ for all couplings, including at the quantum phase transition (QPT) where they are gapless at the wavevector Q of the incipient magnetic order. The excitations of the ordered AF
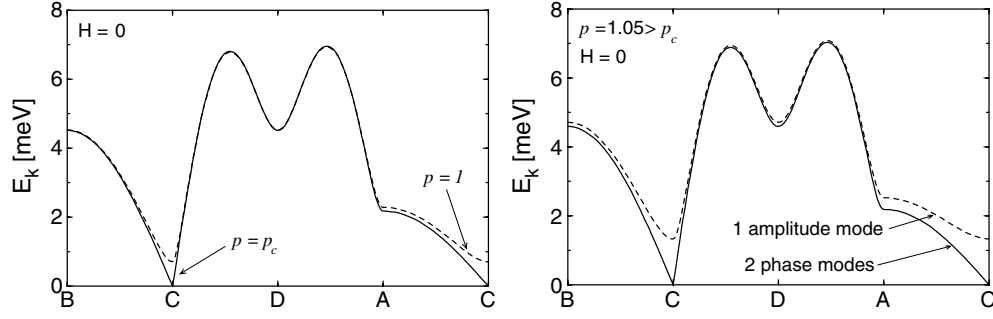
Figure 3. Threefold-degenerate triplet magnon dispersion at zero field. Left: dashed and solid curves correspond respectively to atmospheric ($p = 1$) and critical ($p = p_c \simeq 1.018$) pressures. Right: $p > p_c$, with two degenerate phase modes (solid curve) and one amplitude mode (dashed curve).
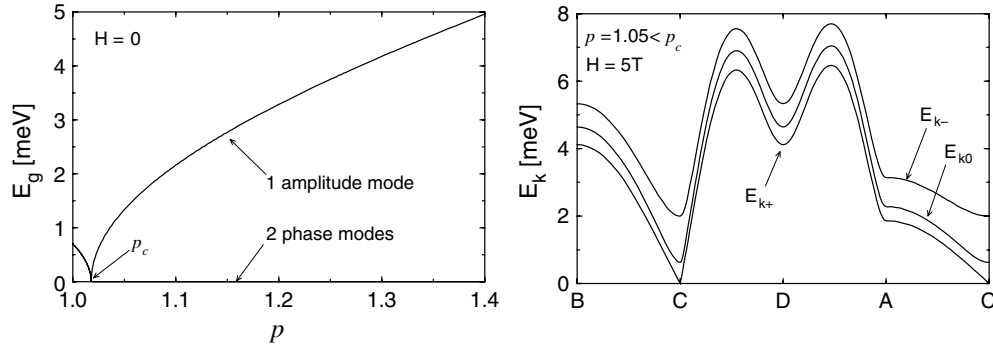

Figure 4. Left: the pressure dependence of spin gaps for phase and amplitude modes. Right: magnon dispersion relations in the pressure-induced AF phase under a magnetic field $H = 5\,\mathrm{T} < H_c$.

phase consist of two spin waves, which are the conventional phase modes (Goldstone modes) of the ordered moment, and a third which corresponds to its amplitude fluctuations and may become low-lying close to the QPT [8].

Structural considerations suggest that the leading effect of applied hydrostatic pressure on TlCuCl$_3$ is to change the interdimer couplings J_2 and J_3,

$$J_2(P) = p(P)J_2, \qquad J_3(P) = p(P)J_3, \qquad (4)$$

where $p(P)$ is a dimensionless function of pressure P, while the relative variation of the dimer and intraladder parameters J and J_1 is minimal. Figure 3 shows that as pressure is raised the bandwidth increases and the spin gap decreases. The magnon modes become soft, $E_Q = 0$, at a critical pressure p_c: for TlCuCl$_3$ the value $p_c = \frac{J - J_1}{J_2 + 2J_3} \simeq 1.018$ represents only a very small fractional increase in p. The dispersion relation at p_c has linear k-dependence around Q (figure 3), in explicit contrast to the case of field-induced order.

Increasing the pressure beyond p_c induces the AF ordered phase, which is described by the operator transformation of equation (3) with $f = g$ at $h = 0$. The modes E_{k0} and E_{k-} remain degenerate and are gapless at Q with linear dispersion around this point. These are the spin waves of the ordered magnet, while the remaining mode, E_{k+}, has a finite gap and corresponds to amplitude fluctuations of the induced moment. The gap for the amplitude mode (figure 4) and the staggered moment of the ordered phase rise monotonically with applied pressure.

Table 1. Exponents for the onset of magnetization.

	$p < p_c$	$p = p_c$	$p > p_c$
M_z	$\gamma = 1$	$\gamma = 3$	$\gamma = 1$
M_{xy}	$\gamma = \frac{1}{2}$	$\gamma = 1$	$\gamma = 2$

At finite pressure and magnetic field the lifting of mode degeneracy is dominated by the field, and the spin waves are no longer equivalent. The right panel of figure 4 shows the dispersion relations for the three nondegenerate modes at a pressure $p > p_c$ for a finite field, where only one Goldstone mode remains. Finally, the uniform and staggered magnetization of TlCuCl$_3$ may also be calculated under finite pressure, and the behaviour is summarized by the exponents γ in table 1, which are obtained near the critical field from the expression $\delta M = M(H) - M(H_c) \propto (H - H_c)^\gamma$. Experimentally, the very small critical pressure in TlCuCl$_3$ means that many experimental probes may be employed to characterize the properties of a significant sample volume on both sides of the QPT, including INS experiments for the observation of the amplitude mode.

5. Bose–Einstein condensation of magnons

The proposal [12] that the magnetic order in TlCuCl$_3$ may be considered as a Bose–Einstein condensation (BEC) of hard-core bosons, or a macroscopic occupation at Q of the soft magnon mode, has motivated extensive studies of the critical properties, particularly the scaling exponent α which determines the power-law dependence

$$T_c(h) \propto |h - h_c|^{1/\alpha} \tag{5}$$

in the vicinity of the QPTs at h_c and h_s. The exponents $\alpha \approx 1.8$–2.6 extracted from various experimental and theoretical studies of KCuCl$_3$ and TlCuCl$_3$ are all larger than the BEC value $\alpha_{BEC} = 3/2$ [12]. While these fits depend critically on data quality and on proximity to the QPT, it is possible that the scaling is not universal, in that α depends on system parameters such as the interdimer interactions. Because the TlCuCl$_3$ structure has no magnetic frustration, the scaling exponent may be studied [13] within a Heisenberg model, $H = \sum_{\langle i,j \rangle} J_{ij} \mathbf{S}_i \cdot \mathbf{S}_j - h \sum_i S_i^z$, where the AF coupling constants J and J' between nearest-neighbour sites i and j denote the intradimer and interdimer interactions for cubic geometry. Taking as the order parameter the staggered magnetization, this may be calculated to high accuracy using the stochastic series expansion quantum Monte Carlo (SSE QMC) method of [14].

Figure 5 shows the critical temperatures $T_c(h)$ obtained for four interdimer coupling ratios, $(J'/J) = 0.07, 0.15, 0.20$ and 0.25, which span the range from narrow-band, large-gap systems to the wide-band, small-gap paradigm. The scaling exponent α in equation (5) is obtained by fitting the data shown in figure 5 with h_c or h_s and α as free parameters. These data are fitted within the varying windows

$$x_1(h) = \frac{h - h_{c1}}{h_{c2} - h_{c1}}, \qquad x_2(h) = \frac{h_{c2} - h}{h_{c2} - h_{c1}}. \tag{6}$$

The dependence on window size x of the exponents α is shown on the right of figure 5. These become smaller as the window size is decreased, and a large window leads to overestimation of α, as also shown by performing the same procedure with the experimental data in panel (a). The extrapolated values approach $\alpha_{BEC} = 1.5$. Higher exponents suggested by previous studies arise from the fitting process, and are in fact consistent with the BEC scenario at the transition. The lines for all interdimer couplings not only scale to the same limit but do so
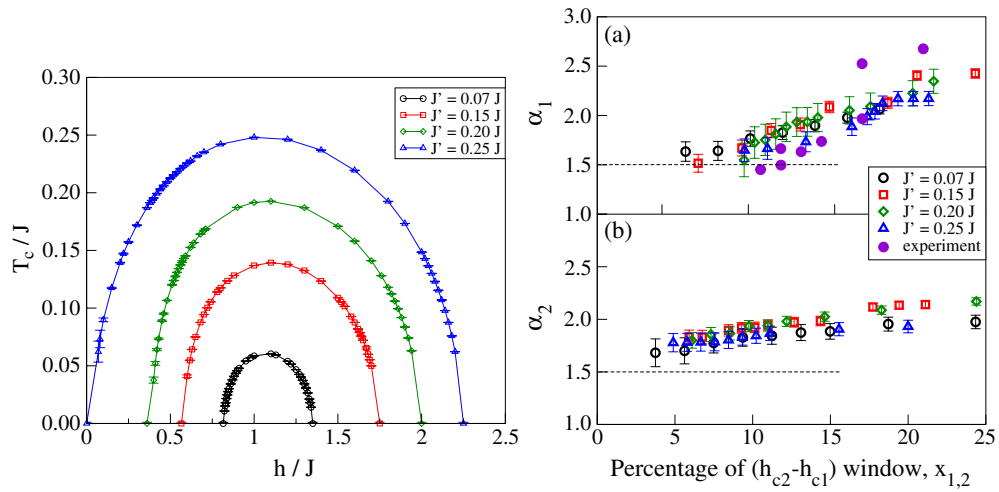
Figure 5. Left: critical temperature for field-induced order in 3d systems of coupled dimers for a range of values of J'. Right: critical exponents α_1 at h_{c1} (a) and α_2 at h_{c2} (b), shown as a function of fitting range x. Filled circles in (a) are experimental data from [4]. Dashed lines mark the BEC result.

(This figure is in colour only in the electronic version)

with the same slope for all x, demonstrating that the critical behaviour is truly universal for all ratios of bandwidth to spin gap. However, universal scaling is obtained only for very narrow windows, and it is not possible to determine a temperature below which true scaling emerges, i.e. the BEC regime is approached only as $T \to 0$. The bond-operator description also shows that the BEC scenario loses validity for fields and temperatures away from the critical point: the macroscopic occupation of one magnon mode mandates a different choice of vacuum (equation (3)) to describe the ground state in the ordered phase.

6. Summary

TlCuCl$_3$ is a 3d coupled-dimer system with a small spin gap which is closed by laboratory pressures and fields. As such it offers a unique opportunity to investigate the phenomena of field- and pressure-induced magnetic order, providing excellent examples of QPTs easily controlled by experiment. A bond-operator description yields a quantitative account of the magnetization and magnon dispersion relations in the ordered phases, and of their continuous evolution through the QPTs. The situation at finite temperatures is best analysed by the numerical SSE QMC technique, which demonstrates the universality of the magnon BEC scenario at the QPT for all coupled-dimer systems. This description is not valid in the ordered regime, which is appropriately considered as a linear combination of dimer singlets and triplets.

References

[1] Takatsu K, Shiramura W and Tanaka H 1997 *J. Phys. Soc. Japan* **66** 1611
[2] Shiramura W, Takatsu K, Tanaka H, Kamishima K, Takahashi M, Mitamura H and Goto T 1997 *J. Phys. Soc. Japan* **66** 1900
[3] Cavadini N, Heigold G, Henggeler W, Furrer A, Güdel H-U, Krämer K and Mutka H 2001 *Phys. Rev.* B **63** 172414

[4] Tanaka H, Oosawa A, Kato T, Uekusa H, Ohashi Y, Kakurai K and Hoser A 2001 *J. Phys. Soc. Japan* **70** 939

[5] Rüegg Ch, Cavadini N, Furrer A, Krämer K, Güdel H-U, Vorderwisch P and Mutka H 2002 *Appl. Phys.* A **74** S840

[6] Rüegg Ch, Cavadini N, Furrer A, Güdel H-U, Krämer K, Mutka H, Wildes A, Habicht K and Vorderwisch P 2003 *Nature* **423** 62

[7] Oosawa A, Fujisawa M, Osakabe T, Kakurai K and Tanaka H 2003 *J. Phys. Soc. Japan* **72** 1026

[8] Normand B and Rice T M 1997 *Phys. Rev.* B **56** 8760

[9] Tanaka H 2003 private communication

[10] Sachdev S and Bhatt R 1990 *Phys. Rev.* B **41** 9323

[11] Matsumoto M, Normand B, Rice T M and Sigrist M 2002 *Phys. Rev. Lett.* **89** 077203

[12] Giamarchi T and Tsvelik A M 1999 *Phys. Rev.* B **59** 11398

[13] Nohadani O, Wessel S, Normand B and Haas S 2003 *Preprint* cond-mat/0307126

[14] Sandvik A W 1999 *Phys. Rev.* B **59** R14157